Chapter 6

A parameter-uniform implicit scheme for two-parameter singularly perturbed parabolic problems

6.1 Introduction

A parameter-uniform implicit scheme for two-parameter singularly perturbed boundary value problems is constructed. Sharp bounds on the solution derivatives are given. The solution is also decomposed into the sum of regular and singular components and the bounds on the derivatives of these components which are used in the convergence analysis are also given. The finite difference scheme on a predefined Shishkin mesh is used to discretize the system of ordinary differential equations in the spatial direction obtained by means of the Crank-Nicolson scheme on an equidistant mesh in the temporal direction. Through rigorous analysis, the theoretical results for two different cases: Case I. $\varepsilon_1/\varepsilon_2^2 \to 0$ as $\varepsilon_2 \to 0$, and Case II. $\varepsilon_2^2/\varepsilon_1 \to 0$ as $\varepsilon_1 \to 0$ which show that the method is convergent irrespective of the size of the parameters $\varepsilon_1, \varepsilon_2$ are provided. The order of accuracy in the first and second cases are shown as $\mathscr{O}((\Delta t)^2 + N^{-1}(\ln N)^2)$ and $\mathscr{O}((\Delta t)^2 + N^{-2}(\ln N)^2)$ respectively. Two test problems are encountered to verify the computational results with theoretical results.

6.2 The Continuous Problem: Preliminaries and a Priori Estimates

Consider the rectangular domain $R = \Omega \times \Lambda$ where $\Omega = (0,1)$, $\Lambda = (0,T]$. The boundary of the domain is $\Gamma = \Gamma_l \cup \Gamma_b \cup \Gamma_r$, where $\Gamma_l = \{(0,t) \mid 0 \le t \le T\}$, $\Gamma_b = \{(x,0) \mid 0 \le$

$x \leq 1\}$ and $\Gamma_r = \{(1,t) \mid 0 \leq t \leq T\}$ are the left, bottom and the right boundaries of R. In this chapter, our aim is to find $\psi(x,t) \in C^{4,2}(R)$ of the following two-parameter singularly perturbed parabolic problems on the rectangular domain R

$$L\psi(x,t) \equiv -\frac{\partial \psi}{\partial t} + \varepsilon_1 \frac{\partial^2 \psi}{\partial x^2} + \varepsilon_2 a(x,t)\frac{\partial \psi}{\partial x} - b(x,t)\psi(x,t) = f(x,t), \quad (x,t) \in R, \tag{6.1a}$$

$$\psi(x,0) = \psi_b(x) \text{ on } \Gamma_b, \tag{6.1b}$$

$$\psi(0,t) = \psi_l(t) \text{ on } \Gamma_l, \tag{6.1c}$$

$$\psi(1,t) = \psi_r(t) \text{ on } \Gamma_r, \tag{6.1d}$$

where $\varepsilon_1, \varepsilon_2$ are two small parameters lying in $(0,1]$. To ensure the existence and uniqueness of the solution of the problem (6.1) the following assumptions are made

- The functions $a(x,t)$, $b(x,t)$, $f(x,t)$ in R and $\psi_l(t)$, $\psi_r(t)$, $\psi_b(x)$ on Γ are bounded and twice continuously differentiable.
- $a(x,t) \geq a^* > 0,\ b(x,t) \geq b^* > 0, \quad (x,t) \in \bar{R}$.
- The initial function satisfies the compatibility conditions at the corner points of the domain.

The summary of the chapter is as follows. Some *a priori* estimates on the solution of the continuous problem are given in Section 6.2. In particular, the bounds of the solution and the minimum principle are given. By decomposing the solution into the smooth and singular components the sharper bounds for the layer components are given for both the cases. In Section 6.3, the temporal discretization by means of the Crank-Nicolson scheme with uniform step size Δt is given and the global error estimate is obtained. Moreover, the system of ODEs obtained in this section is discretized on Shishkin mesh. The main result on the convergence of the proposed method is proved in Section 6.4 followed by the numerical experiments and the discussion on the results in Section 6.5. Finally, some concluding remarks and future considerations are also mentioned in the last Section 6.6.

Some *a priori* estimates, like minimum principle, stability estimate, solution derivatives bounds are established. The proof of the following lemma is standard and is similar to the proof of the maximum principle given in [129].

Lemma 6.2.1. *Let $\Phi \in C^2(R) \cap C^0(\bar{R})$ be non-negative on Γ and $L\Phi$ is non-positive in the interior of R. Then, Φ is non-negative throughout $\bar{R}$.*

Lemma 6.2.2. *The parameter-uniform estimate on $\psi(x,t)$ is given by*

$$\|\psi\|_{\bar{R}} \leq \|\psi\|_{\Gamma} + \frac{\|f\|_{\bar{R}}}{b^*}.$$

Proof. It is easy to verify that the barrier functions $\Pi^{\pm}(x,t) = \|\psi\|_{\Gamma} + \frac{\|f\|_{\bar{R}}}{b^*} \pm \psi(x,t)$ are non-negative on Γ. Also, at an interior point (x,t) of R

$$L\Pi^{\pm}(x,t) = -b\left[\|\psi\|_{\Gamma} + \frac{\|f\|_{\bar{R}}}{b^*}\right] \pm L\psi(x,t) \leq -b^*\|\psi\|_{\Gamma} - \|f\|_{\bar{R}} \pm f \leq -\|f\|_{\bar{R}} \pm f \leq 0.$$

The proof is completed by using the minimum principle. □

Now we decompose the solution ψ of the problem (6.1) into the regular and singular components (in both cases), which will be used in the error analysis. **Case I.** $\varepsilon_1/\varepsilon_2^2 \to 0$ as $\varepsilon_2 \to 0$. In this case, the decomposition is as follows:

$$\psi = U + V + W,$$

where the regular component U and the left and right singular components V and W satisfy the following BVP.

$$\begin{aligned}
&LU = f, \quad U(0,t),\ U(1,t) \text{ chosen suitably, and } U(x,0) = \psi_b(x),\\
&LV = 0, \quad V(0,t) = \psi_l(t) - U(0,t) - W(0,t),\ V(1,t) \text{ chosen suitably},\\
&\quad V(x,0) = 0,\\
&LW = 0, \quad W(0,t) \text{ chosen suitably}, W(1,t) = \psi_r(t) - U(1,t) - V(1,t),\\
&\quad W(x,0) = 0.
\end{aligned}$$

Lemma 6.2.3. *The layer components V, W satisfy the following bounds:*

$$\begin{aligned}
&|V(x,t)| \leq C\exp((-a^*\varepsilon_2/\varepsilon_1)x),\\
&|W(x,t)| \leq C\exp((-b^*/\varepsilon_2)(1-x)).
\end{aligned}$$

Proof. The proof can be done by following the approach given in [105]. □

The bounds for the smooth and singular components are given by the following theorem.

Theorem 6.2.1. *For the non-negative integers i, j satisfying $0 \leq i+3j \leq 4$, the components in case I satisfy the following bounds.*

$$\left\| \frac{\partial^{i+j} U}{\partial x^i \partial t^j} \right\|_{\overline{R}} \leq C\left(1+(\varepsilon_1/\varepsilon_2)^{3-i}\right),$$
$$\left\| \frac{\partial^{i+j} V}{\partial x^i \partial t^j} \right\|_{\overline{R}} \leq C(\varepsilon_2/\varepsilon_1)^i,$$
$$\left\| \frac{\partial^{i+j} W}{\partial x^i \partial t^j} \right\|_{\overline{R}} \leq C\varepsilon_2^{-i}.$$

Proof. The proof can be done by following the approach given in [131]. □

Case II. $\varepsilon_2^2/\varepsilon_1 \to 0$ as $\varepsilon_1 \to 0$. In this case, the decomposition is as follows:

$$\psi = \chi + Z,$$

where the regular and singular components χ and Z, respectively satisfy

$$L\chi = f, \quad \chi(0,t), \chi(1,t) \text{ chosen suitably,}$$
$$LZ = 0, \quad Z(0,t) = \psi_l(t) - \chi(0,t),\ Z(1,t) = \psi_r(t) - \chi(1,t).$$

Lemma 6.2.4. *For some $0 < \delta \leq 1/2$, the layer component satisfies*

$$|Z(x,t)| \leq C\exp\left(\left(-\sqrt{\gamma b^*/\varepsilon_1}\right)x\right), \quad x \in [0,\delta],$$
$$|Z(x,t)| \leq C\exp\left(\left(-\sqrt{\gamma b^*/\varepsilon_1}\right)(1-x)\right), \quad x \in [1-\delta,1],$$

where the constant γ is given by $\gamma = \min\limits_{(x,t)\in R}\left\{\dfrac{b(x,t)}{a(x,t)}\right\}$.

Proof. The proof can be done by following the approach given in [105]. □

The bounds on the derivatives of the smooth and singular components are given by the following theorem.

Theorem 6.2.2. *For the non-negative integers i, j satisfying $0 \le i+3j \le 4$, the components in Case II satisfy the following bounds.*

$$\left\| \frac{\partial^{i+j}\chi}{\partial x^i \partial t^j} \right\|_{\overline{R}} \le C\left(1+\varepsilon_1^{-(i-3)/2}\right),$$
$$\left\| \frac{\partial^{i+j}Z}{\partial x^i \partial t^j} \right\|_{\overline{R}} \le C\varepsilon_1^{-i/2}.$$

Proof. The proof can be done by following the approach given in [131]. □

6.3 The Proposed Scheme

Based on the Crank-Nicolson method an implicit numerical scheme to solve (6.1) is introduced in this section. The following uniform mesh Λ^M in the temporal direction is obtained by dividing the time interval $[0,T]$ into M partitions each of width Δt

$$\Lambda^M = \left\{ t_n = n\Delta t : \ n = 0,1,\ldots,M, \Delta t = \tfrac{T}{M} \right\}.$$

Then on $\Omega \times \Lambda^M$ problem (6.1) is semi-discretized as follows

$$\begin{aligned} -D_t^- Y^{n+1}(x) + \varepsilon_1 (Y_{xx})^{n+1/2} + \varepsilon_2 a^{n+1}(x)(Y_x)^{n+1/2} - b^{n+1}(x)Y^{n+1/2} &= f^{n+1}(x), \\ x \in \Omega,\ 0 \le n \le M-1, & \\ Y^{n+1}(0) = \psi_l(t_{n+1}),\ Y^{n+1}(1) = \psi_r(t_{n+1}), \quad 0 \le n \le M-1, & \\ Y^0(x) = \psi_b(x), \quad x \in \Omega, & \end{aligned}$$

where $Y^{n+1}(x)$ is the approximation of $\psi(x,t_{n+1})$ at $(n+1)$-th time level, D_t^- is the backward difference operator, $v^{n+1/2}(x) = \frac{v^{n+1}(x)+v^n(x)}{2}$, and $a^{n+1}(x) = a(x,t_{n+1})$, $b^{n+1}(x) = b(x,t_{n+1})$, $f^{n+1}(x) = f(x,t_{n+1})$. Rewriting the above equation as

$$\begin{cases} \hat{L}Y^{n+1}(x) = g(x,t_{n+1}), & x \in \Omega,\ 0 \le n \le M-1, \\ Y^{n+1}(0) = \psi_l(t_{n+1}),\ Y^{n+1}(1) = \psi_r(t_{n+1}), & 0 \le n \le M-1, \\ Y^0(x) = \psi_b(x), \quad x \in \Omega, & \end{cases} \tag{6.2}$$

where the operator $\hat{L}$ is given by

$$\hat{L} \equiv \frac{\varepsilon_1}{2}\frac{d^2}{dx^2} + \varepsilon_2 \frac{a^{n+1}(x)}{2}\frac{d}{dx} - \frac{c^{n+1}(x)}{2} I,$$

and

$$\begin{aligned} g(x,t_{n+1}) &= f^{n+1}(x) - \frac{\varepsilon_1}{2}(Y_{xx})^n(x) - \varepsilon_2 \frac{a^{n+1}(x)}{2}(Y_x)^n(x) + \frac{d^{n+1}(x)}{2} Y^n(x), \\ c^{n+1}(x) &= b^{n+1}(x) + \frac{2}{\Delta t}, \\ d^{n+1}(x) &= b^{n+1}(x) - \frac{2}{\Delta t}. \end{aligned}$$

Depending on the values of ε_1 and ε_2, in Case I *i.e.,* $\varepsilon_1/\varepsilon_2^2 \to 0$ as $\varepsilon_2 \to 0$, the solution of (6.2) can be decomposed as

$$\underbrace{Y^{n+1}(x)}_{\text{Solution}} = \underbrace{U^{n+1}(x)}_{\text{Regular component}} + \underbrace{V^{n+1}(x)}_{\text{Left singular component}} + \underbrace{W^{n+1}(x)}_{\text{Right singular component}},$$

while in Case II *i.e.,* $\varepsilon_2^2/\varepsilon_1 \to 0$ as $\varepsilon_1 \to 0$, the solution decomposition is as given below

$$\underbrace{Y^{n+1}(x)}_{\text{Solution}} = \underbrace{\chi^{n+1}(x)}_{\text{Regular component}} + \underbrace{Z^{n+1}(x)}_{\text{Singular component}}.$$

The bounds for these smooth and singular components are given same as given in Theorems 6.2.1 and 6.2.2. The operator $\hat{L}$ in (6.2) satisfies the following minimum principle.

Lemma 6.3.1 (Minimum Principle)**.** *Let* $\Phi^{n+1}(0) \geq 0, \Phi^{n+1}(1) \geq 0$ *and* $\hat{L}\Phi^{n+1}(x) \leq 0$ *for all* $x \in \Omega$ *then* $\Phi^{n+1}(x) \geq 0$ *for all* $x \in \bar{\Omega}$.

Proof. For contrary suppose for some $\xi \in \Omega$, $\Phi^{n+1}(\xi) = \min_{x\in\Omega} \Phi^{n+1}(x) < 0$. Then,

$$\hat{L}\Phi^{n+1}(\xi) = \frac{\varepsilon_1}{2}(\Phi^{n+1})_{xx}(\xi) + \varepsilon_2 \frac{a^{n+1}(\xi)}{2}(\Phi^{n+1})_x(\xi) - \frac{c^{n+1}(\xi)}{2}\Phi^{n+1}(\xi) > 0,$$

as $c^{n+1}(\xi) > 0$. Hence, the proof is completed. □

The following lemma estimates the local truncation error T_{n+1} in the temporal semi-discretization (6.2).

Lemma 6.3.2. *The local error T_{n+1} satisfy*

$$\|T_{n+1}\| \leq C(\Delta t)^3.$$

Proof. Using Taylor's theorem, we have

$$\psi(x,t_{n+1}) = \psi(x,t_{n+1/2}) + \frac{\Delta t}{2}\psi_t(x,t_{n+1/2}) + \frac{(\Delta t)^2}{8}\psi_{tt}(x,t_{n+1/2}) + O((\Delta t)^3),$$
$$\psi(x,t_n) = \psi(x,t_{n+1/2}) - \frac{\Delta t}{2}\psi_t(x,t_{n+1/2}) + \frac{(\Delta t)^2}{8}\psi_{tt}(x,t_{n+1/2}) + O((\Delta t)^3).$$

On subtracting, it gives

$$\begin{aligned}\frac{\psi(x,t_{n+1}) - \psi(x,t_n)}{\Delta t} &= \psi_t\left(x,t_{n+1/2}\right) + O((\Delta t)^2)\\ &= \varepsilon_1\psi_{xx}\left(x,t_{n+1/2}\right) + \varepsilon_2 a\left(x,t_{n+1/2}\right)\psi_x\left(x,t_{n+1/2}\right)\\ &\quad - b\left(x,t_{n+1/2}\right)\psi\left(x,t_{n+1/2}\right) - f\left(x,t_{n+1/2}\right) + O((\Delta t)^2),\end{aligned}$$

where $a\left(x,t_{n+1/2}\right) = \frac{a(x,t_{n+1})+a(x,t_n)}{2} + O((\Delta t)^2)$, etc. So, we can see that the local error is the solution of

$$\hat{L}T_{n+1} = O((\Delta t)^3),\ T_{n+1}(0) = T_{n+1}(1) = 0.$$

Hence, by using the minimum principle we get the required result. □

Lemma 6.3.3. *The global error E_n is estimated as*

$$\|E_n\| \leq C(\Delta t)^2, \quad 0 \leq n \leq M.$$

Proof. The contribution of the truncation errors and using local error estimate given in Lemma 6.3.2 gives the required estimate. □

The solutions $\eta_0(x) < 0$ and $\eta_1(x) > 0$ of the characteristic equation

$$\varepsilon_1\lambda^2(x) + \varepsilon_2 a(x)\lambda(x) - c(x) = 0,$$

characterize the layer behavior of the solution. More precisely,

$$\mu_0 = -\max_{x\in[0,1]}\eta_0(x),\ \text{and}\ \mu_1 = \min_{x\in[0,1]}\eta_1(x),$$

describe the boundary layer width and the rate at which the solution decay/rise in the layer region. Due to the presence of the boundary layers, one can not achieve the uniform convergence on an equidistant mesh. Therefore, the method is applied to a mesh which is dense in layer regions. Let $N \geq 4$ be the number of mesh intervals used. To construct the mesh the interval $[0,1]$ is divided into three sub-intervals $\Omega_1 = [0, \sigma_1]$, $\Omega_2 = (\sigma_1, 1-\sigma_2]$, and $\Omega_3 = (1-\sigma_2, 1]$ where the transition parameters σ_1 and σ_2 are defined as

$$\sigma_1 = \min\left\{\frac{1}{4}, \frac{\ln N}{\mu_0}\right\}, \quad \sigma_2 = \min\left\{\frac{1}{4}, \frac{\ln N}{\mu_1}\right\}.$$

In Case I, we have taken $\mu_0 = a^*\varepsilon_2/\varepsilon_1$, $\mu_1 = \gamma/\varepsilon_2$, while in Case II, we have taken $\mu_0 = \sqrt{a^*\gamma/\varepsilon_1}$, and $\mu_1 = \sqrt{a^*\gamma/\varepsilon_1}$. We define the fitted piecewise-uniform mesh $\Omega^N = \{x_i\}_{i=0}^N$ as

$$x_i = \begin{cases} \dfrac{4\sigma_1}{N} i, & \text{if} \quad i = 0, 1, \ldots, \dfrac{N}{4}, \\ \sigma_1 + \dfrac{2(1-\sigma_1-\sigma_2)}{N}\left(i - \dfrac{N}{4}\right), & \text{if} \quad i = \dfrac{N}{4}+1, \ldots, \dfrac{3N}{4}, \\ (1-\sigma_2) + \dfrac{4\sigma_2}{N}\left(i - \dfrac{3N}{4}\right), & \text{if} \quad i = \dfrac{3N}{4}+1, \ldots, N, \end{cases}$$

and the mesh spacing is given by

$$h_i = x_i - x_{i-1} = \begin{cases} H_1 = \dfrac{4\sigma_1}{N}, & \text{if} \quad i = 1, 2, \ldots, \dfrac{N}{4}, \\ H_2 = \dfrac{2(1-\sigma_1-\sigma_2)}{N}, & \text{if} \quad i = \dfrac{N}{4}+1, \ldots, \dfrac{3N}{4}, \\ H_3 = \dfrac{4\sigma_2}{N}, & \text{if} \quad i = \dfrac{3N}{4}+1, \ldots, N. \end{cases}$$

Note that in Case I, the values of σ_1 and σ_2 are different while in Case II, the width of both boundary layers are of same order and so we have $\sigma_1 = \sigma_2$. Also, the mesh is uniform when $\sigma_1 = \sigma_2 = 1/4$ otherwise, the mesh is dense in layer regions. The fitted-piecewise-uniform mesh $R^{N,M}$ on R is then defined as the tensor product $\Omega^N \times \Lambda^M$. The boundary points $\Gamma^{N,M}$ on $R^{N,M}$ are given by $\Gamma^{N,M} = \bar{R}^{N,M} \cap \Gamma$. Introducing the operators

$$D_x^- \mu_i^n = \frac{\mu_i^n - \mu_{i-1}^n}{h_i}, \; D_x^+ \mu_i^n = \frac{\mu_{i+1}^n - \mu_i^n}{h_{i+1}}, \; \delta_x^2 \mu_i^n = \frac{(D_x^+ - D_x^-)\mu_i^n}{i},$$

where $_i = \frac{h_i+h_{i+1}}{2}$, the full discretization of (6.2) on $R^{N,M}$ is given by

$$\begin{cases} \mathscr{L}^N \widetilde{\psi}(x_i) = \widetilde{g}(x_i), \quad x_i \in \Omega^N, \\ \widetilde{\psi}(x_0) = \psi_l(t_{n+1}), \quad \widetilde{\psi}(x_N) = \psi_r(t_{n+1}), \quad 0 \le n \le M-1, \end{cases} \tag{6.3}$$

where $\widetilde{\psi}(x_i)$ is the approximation of $Y^{n+1}(x_i)$ and the operator $\mathscr{L}^N$ is defined as

$$\mathscr{L}^N \widetilde{\psi} :\equiv \frac{\varepsilon_1}{2}\delta_x^2 \widetilde{\psi} + \varepsilon_2 \frac{a^{n+1}}{2} D_x^- \widetilde{\psi} - \frac{c^{n+1}}{2}\widetilde{\psi}.$$

Moreover, the function $\widetilde{g}(x_i)$ is given by

$$\widetilde{g}(x_i) = f^{n+1}(x_i) - \frac{\varepsilon_1}{2}\delta_x^2 Y^n(x_i) - \varepsilon_2 \frac{a^{n+1}(x_i)}{2} D_x^- Y^n(x_i) + \frac{d^{n+1}(x_i)}{2} Y^n(x_i).$$

Lemma 6.3.4. *The following are the bounds on an arbitrary mesh and uniform mesh respectively*

$$\left|\left(\mathscr{L}^N - \hat{L}\right)\psi\right| \le C(\varepsilon_1 h_i |\psi|_3 + \varepsilon_2 h_i \|a\| |\psi|_2),$$
$$\left|\left(\mathscr{L}^N - \hat{L}\right)\psi\right| \le C(\varepsilon_1 h^2 |\psi|_4 + \varepsilon_2 h \|a\| |\psi|_2).$$

Proof. Taylor series expansion gives

$$\psi(x_{i+1},t_{n+1}) = \psi(x_i,t_{n+1}) + h_{i+1}\psi'(x_i,t_{n+1}) + \frac{h_{i+1}^2}{2}\psi''(x_i,t_{n+1}) + \frac{h_{i+1}^3}{6}\psi'''(x_i,t_{n+1}) + \frac{h_{i+1}^4}{24}\psi^{(4)}(x_i,t_{n+1}) + \cdots, \tag{6.4}$$

$$\psi(x_{i-1},t_{n+1}) = \psi(x_i,t_{n+1}) - h_i\psi'(x_i,t_{n+1}) + \frac{h_i^2}{2}\psi''(x_i,t_{n+1}) - \frac{h_i^3}{6}\psi'''(x_i,t_{n+1}) + \frac{h_i^4}{24}\psi^{(4)}(x_i,t_{n+1}) + \cdots. \tag{6.5}$$

Equation (6.4) gives

$$\begin{aligned} D_x^+\psi(x_i,t_{n+1}) &= \frac{\psi(x_{i+1},t_{n+1}) - \psi(x_i,t_{n+1})}{h_{i+1}} \\ &= \psi'(x_i,t_{n+1}) + \frac{h_{i+1}}{2}\psi''(x_i,t_{n+1}) + \frac{h_{i+1}^2}{6}\psi'''(x_i,t_{n+1}) \\ &\quad + \frac{h_{i+1}^3}{24}\psi^{(4)}(x_i,t_{n+1}) + \cdots, \end{aligned} \tag{6.6}$$

and Equation (6.5) gives

$$\begin{aligned} D_x^- \psi(x_i,t_{n+1}) &= \frac{\psi(x_i,t_{n+1})-\psi(x_{i-1},t_{n+1})}{h_i} \\ &= \psi'(x_i,t_{n+1}) - \frac{h_i}{2}\psi''(x_i,t_{n+1}) + \frac{h_i^2}{6}\psi'''(x_i,t_{n+1}) - \frac{h_i^3}{24}\psi^{(4)}(x_i,t_{n+1}) \\ &\quad + \cdots, \end{aligned} \tag{6.7}$$

or

$$D_x^- \psi(x_i,t_{n+1}) - \psi'(x_i,t_{n+1}) = -\frac{h_i}{2}\psi''(x_i,t_{n+1}) + \frac{h_i^2}{6}\psi'''(x_i,t_{n+1}) - \frac{h_i^3}{24}\psi^{(4)}(x_i,t_{n+1}) + \cdots. \tag{6.8}$$

On subtracting (6.7) from (6.6),

$$\begin{aligned} D_x^+ \psi(x_i,t_{n+1}) - D_x^- \psi(x_i,t_{n+1}) &= \frac{h_{i+1}+h_i}{2}\psi''(x_i,t_{n+1}) + \frac{h_{i+1}^2-h_i^2}{6}\psi'''(x_i,t_{n+1}) \\ &\quad + \frac{h_{i+1}^3+h_i^3}{24}\psi^{(4)}(x_i,t_{n+1}) + \cdots \\ &=_i \psi''(x_i,t_{n+1}) + \frac{h_{i+1}-h_i}{3}{}_i\,\psi'''(x_i,t_{n+1}) \\ &\quad + \frac{(h_{i+1}^2+h_i^2-h_ih_{i+1})}{12}{}_i\,\psi^{(4)}(x_i,t_{n+1}) + \cdots, \end{aligned}$$

and so,

$$\begin{aligned} \delta_x^2 \psi(x_i,t_{n+1}) - \psi''(x_i,t_{n+1}) &= \frac{h_{i+1}-h_i}{3}\psi'''(x_i,t_{n+1}) \\ &\quad + \frac{(h_{i+1}^2+h_i^2-h_ih_{i+1})}{12}\psi^{(4)}(x_i,t_{n+1}) + \cdots. \end{aligned} \tag{6.9}$$

Now

$$\begin{aligned} (L^N - \hat{L})\psi(x_i,t_{n+1}) &= \frac{\varepsilon_1}{2}\left(\delta_x^2\psi(x_i,t_{n+1}) - \psi''(x_i,t_{n+1})\right) \\ &\quad + \varepsilon_2 \frac{a^{n+1}(x)}{2}\left(D_x^-\psi(x_i,t_{n+1}) - \psi'(x_i,t_{n+1})\right). \end{aligned} \tag{6.10}$$

Use of (6.8) and (6.9) on arbitrary and uniform mesh gives the required result. □

6.4 Parameter Uniform Convergence Analysis

Before proving the main result on the convergence of the proposed method we give some basic properties satisfy by the operator $\mathscr{L}^N$.

Lemma 6.4.1. *Assume that* $\widetilde{\Phi}(x_0) \geq 0, \widetilde{\Phi}(x_N) \geq 0$ *and* $\mathscr{L}^N\widetilde{\Phi}(x_i) \leq 0$ *for all* $x_i \in \Omega^N$ *then* $\widetilde{\Phi}(x_i) \geq 0$ *for all* $x_i \in \Omega^N$.

Proof. If $\widetilde{\Phi}(q_i) = \min_{x_i \in \Omega^N} \widetilde{\Phi}(x_i) < 0$ for some $q_i \in \Omega^N$, then

$$\begin{aligned}
\mathscr{L}^N\widetilde{\Phi}(q_i) &= \frac{\varepsilon_1}{2}\delta_x^2\widetilde{\Phi}(q_i) + \varepsilon_2\frac{a^{n+1}(q_i)}{2}D_x^-\widetilde{\Phi}(q_i) - \frac{c^{n+1}(q_i)}{2}\widetilde{\Phi}(q_i) \\
&= \frac{\varepsilon_1}{2_i}\left(\frac{\widetilde{\Phi}(q_{i+1}) - \widetilde{\Phi}(q_i)}{h_{i+1}} - \frac{\widetilde{\Phi}(q_i) - \widetilde{\Phi}(q_{i-1})}{h_i}\right) \\
&+ \varepsilon_2\frac{a^{n+1}(q_i)}{2}\left(\frac{\widetilde{\Phi}(q_i) - \widetilde{\Phi}(q_{i-1})}{h_i}\right) - \frac{c^{n+1}(q_i)}{2}\widetilde{\Phi}(q_i) \\
&> 0,
\end{aligned}$$

which contradicts the hypothesis and hence the proof is completed. □

Lemma 6.4.2. *Any mesh function* $\widetilde{\Phi}(x)$ *which vanishes at the boundary points satisfies*

$$\left|\widetilde{\Phi}(x_i)\right| \leq \max_{x_i \in \Omega^N}\left|\mathscr{L}^N\widetilde{\Phi}(x_i)\right|, \; x_i \in \Omega^N.$$

Proof. For the barrier functions $\Psi^{\pm}(x_i) = \max_{x_i \in \Omega^N}\left|\mathscr{L}^N\widetilde{\Phi}(x_i)\right| \pm \widetilde{\Phi}(x_i)$, we have

$$\begin{aligned}
\Psi^{\pm}(x_0) &= \max_{x_i \in \Omega^N}\left|\mathscr{L}^N\widetilde{\Phi}(x_i)\right| \pm \widetilde{\Phi}(x_0) = \max_{x_i \in \Omega^N}\left|\mathscr{L}^N\widetilde{\Phi}(x_i)\right| \geq 0, \\
\Psi^{\pm}(x_N) &= \max_{x_i \in \Omega^N}\left|\mathscr{L}^N\widetilde{\Phi}(x_i)\right| \pm \widetilde{\Phi}(x_N) = \max_{x_i \in \Omega^N}\left|\mathscr{L}^N\widetilde{\Phi}(x_i)\right| \geq 0.
\end{aligned}$$

Also, at the intermediate points

$$\begin{aligned}
\mathscr{L}^N\Psi^{\pm}(x_i) &= \mathscr{L}^N\left[\max_{x_i\in\Omega^N}\left|\mathscr{L}^N\widetilde{\Phi}(x_i)\right| \pm \widetilde{\Phi}(x_i)\right] \\
&= -\frac{c^{n+1}(x_i)}{2}\max_{x_i\in\Omega^N}\left|\mathscr{L}^N\widetilde{\Phi}(x_i)\right| \pm \mathscr{L}^N\widetilde{\Phi}(x_i) \\
&= -\frac{1}{2}\left(b^{n+1}(x_i)+\frac{2}{\Delta t}\right)\max_{x_i\in\Omega^N}\left|\mathscr{L}^N\widetilde{\Phi}(x_i)\right| \pm \mathscr{L}^N\widetilde{\Phi}(x_i) \\
&\leq \left(\frac{-b^*}{2}-\frac{1}{\Delta t}\right)\max_{x_i\in\Omega^N}\left|\mathscr{L}^N\widetilde{\Phi}(x_i)\right| \pm \mathscr{L}^N\widetilde{\Phi}(x_i) \\
&\leq -\left|\mathscr{L}^N\widetilde{\Phi}(x_i)\right| \pm \mathscr{L}^N\widetilde{\Phi}(x_i) \\
&\leq 0.
\end{aligned}$$

An application of Lemma 6.4.1 yields the required result. □

We shall now prove the convergence of the proposed scheme for both cases separately.

Analysis for Case I ($\varepsilon_1/\varepsilon_2^2 \to 0$ as $\varepsilon_2 \to 0$). In this case, we decompose the solution $\widetilde{\psi}_i$ of (6.3) into the regular and singular components as

$$\underbrace{\widetilde{\psi}_i}_{\text{Solution}} = \underbrace{\widetilde{U}_i}_{\text{Regular component}} + \underbrace{\widetilde{V}_i}_{\text{Left singular component}} + \underbrace{\widetilde{W}_i}_{\text{Right singular component}},$$

where the regular component $\widetilde{U}_i$ satisfies the following in-homogeneous problem

$$\mathscr{L}^N\widetilde{U}_i = \widetilde{g}(x_i) \text{ in } R^{N,M}, \quad \widetilde{U}_i = U^{n+1}(x_i) \text{ on } \Gamma^{N,M},$$

and the singular components $\widetilde{V}_i$ and $\widetilde{W}_i$ satisfy the following homogeneous problem

$$\mathscr{L}^N\widetilde{V}_i = 0 \text{ in } R^{N,M}, \quad \widetilde{V}_i = V^{n+1}(x_i) \text{ on } \Gamma^{N,M},$$

$$\mathscr{L}^N\widetilde{W}_i = 0 \text{ in } R^{N,M}, \quad \widetilde{W}_i = W^{n+1}(x_i) \text{ on } \Gamma^{N,M}.$$

Thus, the nodal error is given by

$$v_{i,n+1} = \psi(x_i,t_{n+1}) - \widetilde{\psi}_i = (U^{n+1}(x_i)-\widetilde{U}_i) + (V^{n+1}(x_i)-\widetilde{V}_i) + (W^{n+1}(x_i)-\widetilde{W}_i).$$

Furthermore, the bounds for the singular components are given by the following theorem.

Theorem 6.4.1. *The bounds on the components are given as*

$$\left|\widetilde{V}_i\right| \leq C\prod_{j=1}^{i}\left(1+\mu_0 h_j\right)^{-1}, \quad |\widetilde{V}_0| \leq C,$$
$$\left|\widetilde{W}_i\right| \leq C\prod_{j=i+1}^{N}\left(1+\mu_1 h_j\right)^{-1}, \quad |\widetilde{W}_N| \leq C.$$

Proof. The proof can be done by following the approach given in [105]. □

Lemma 6.4.3. *The error bound for the regular component is given by*

$$\left\|U^{n+1}(x_i)-\widetilde{U}_i\right\|_{\Omega^N} \leq CN^{-2}.$$

Proof. Using the classical argument, we obtain

$$\begin{aligned}\left|\mathscr{L}^N\left(U^{n+1}(x_i)-\widetilde{U}_i\right)\right| &= \left|\mathscr{L}^N U^{n+1}(x_i)-\widetilde{g}(x_i)\right| \\ &= \left|\mathscr{L}^N U^{n+1}(x_i)-g(x_i,t_{n+1})+g(x_i,t_{n+1})-\widetilde{g}(x_i)\right| \\ &= \left|\mathscr{L}^N U^{n+1}(x_i)-\hat{L}U^{n+1}(x_i)+g(x_i,t_{n+1})-\widetilde{g}(x_i)\right| \\ &\leq \left|\mathscr{L}^N U^{n+1}(x_i)-\hat{L}U^{n+1}(x_i)\right|+\left|g(x_i,t_{n+1})-\widetilde{g}(x_i)\right|.\end{aligned} \tag{6.11}$$

Now, we have

$$\begin{aligned}\widetilde{g}(x_i)-g(x_i,t_{n+1}) &= \frac{\varepsilon_1}{2}\left(\delta_x^2 Y^n(x_i)-(Y^n)_{xx}(x_i)\right)+\varepsilon_2\frac{a^{n+1}(x)}{2}\left(D_x^- Y^n(x_i)-(Y^n)_x(x_i)\right) \\ &= \left(\mathscr{L}^N-\hat{L}\right)Y^n(x_i), \quad \text{(using Eq. (6.10))}\end{aligned}$$

and so, (6.11) gives

$$\left|\mathscr{L}^N\left(U^{n+1}(x_i)-\widetilde{U}_i\right)\right| \leq \left|\left(\mathscr{L}^N-\hat{L}\right)U^{n+1}(x_i)\right|+\left|\left(\mathscr{L}^N-\hat{L}\right)Y^n(x_i)\right|.$$

Using Lemma 6.3.4 which gives

$$\begin{aligned}\left|\mathscr{L}^N\left(U^{n+1}(x_i)-\widetilde{U}_i\right)\right| &\leq C_1\left(\varepsilon_1 N^{-2}|U^{n+1}|_4+\varepsilon_2 N^{-1}\|a\||U^{n+1}|_2\right) \\ &\quad +C_2\left(\varepsilon_1 N^{-2}|Y^n|_4+\varepsilon_2 N^{-1}\|a\||Y^n|_2\right) \\ &\leq CN^{-2}.\end{aligned}$$

Thus, an application of Lemma 6.4.2 gives

$$\left\| U^{n+1}(x_i) - \widetilde{U}_i \right\|_{\Omega^N} \leq CN^{-2}. \qquad \square$$

Lemma 6.4.4. *The error bound for the left singular component is given by*

$$\left\| V^{n+1}(x_i) - \widetilde{V}_i \right\|_{\Omega^N} \leq CN^{-1}(\ln N)^2.$$

Proof. In the case $\sigma_1 = \sigma_2 = 1/4$, we have $\varepsilon_2/\varepsilon_1 \leq C \ln N$ and so using the classical argument, we obtain

$$\begin{aligned}
\left| \mathscr{L}^N \left(V^{n+1}(x_i) - \widetilde{V}_i \right) \right| &= \left| \mathscr{L}^N V^{n+1}(x_i) - 0 \right| \\
&= \left| \left(\mathscr{L}^N - \hat{L} \right) V^{n+1}(x_i) \right| \\
&\leq C \left(\varepsilon_1 h^2 \left| V^{n+1}(x_i) \right|_4 + \varepsilon_2 h \|a\| \left| V^{n+1}(x_i) \right|_2 \right) \\
&\leq CN^{-2}.
\end{aligned}$$

On the other hand, in the latter case $\sigma_1 = \sigma_2 < 1/4$, for $x_i \in [0, \sigma_1)$ the classical argument as used above gives

$$\begin{aligned}
\left| \mathscr{L}^N \left(V^{n+1}(x_i) - \widetilde{V}_i \right) \right| &\leq C \left(\varepsilon_1 H_1^2 \left| V^{n+1}(x_i) \right|_4 + \varepsilon_2 H_1 \|a\| \left| V^{n+1}(x_i) \right|_2 \right) \\
&\leq C \left(\varepsilon_1 \sigma_1^2 N^{-2} \left| V^{n+1}(x_i) \right|_4 + \varepsilon_2 \sigma_1 N^{-1} \|a\| \left| V^{n+1}(x_i) \right|_2 \right) \\
&\leq \frac{\varepsilon_2^2}{\varepsilon_1} N^{-1} \ln N.
\end{aligned}$$

Now consider $\Phi(x) = C \left(N^{-1} + N^{-1} \ln N (\sigma_1 - x)(\varepsilon_2/\varepsilon_1) \right)$. Then

$$\mathscr{L}^N \Phi_i = - \left(c^{n+1} \Phi_i + C \varepsilon_2^2 / \varepsilon_1 (N^{-1} \ln N) \right) \leq - \left| \mathscr{L}^N \left(V^{n+1}(x_i) - \widetilde{V}_i \right) \right|.$$

An application of the discrete minimum principle yields

$$\begin{aligned}
\left| V^{n+1}(x_i) - \widetilde{V}_i \right| &= C \left(N^{-1} + (N^{-1} \ln N)(\sigma_1 - x_i)(\varepsilon_2/\varepsilon_1) \right) \\
&\leq C \left(N^{-1} + (N^{-1} \ln N) \sigma_1 (\varepsilon_2/\varepsilon_1) \right) \\
&\leq CN^{-1}(\ln N)^2. \qquad (6.12)
\end{aligned}$$

Furthermore, for $x_i \in [\sigma_1, 1]$, we have

$$\left|V^{n+1}(x_i) - \widetilde{V}_i\right| \leq \left|V^{n+1}(x_i)\right| + \left|\widetilde{V}_i\right|$$

Using Theorem 6.4.1, we get

$$\left|\widetilde{V}_{N/4}\right| \leq C\left(1 + 4N^{-1}\ln N\right)^{-N/4}.$$

Now the inequality $\ln(1+x) > x(1-x/2)$ for $x = 4N^{-1}\ln N$ gives $\left|\widetilde{V}_i\right| \leq CN^{-1}$, $\forall x_i \in [\sigma_1, 1]$. Also,

$$\begin{aligned}\left|V^{n+1}(x_i)\right| &\leq C\exp(-(a^*\varepsilon_2/\varepsilon_1)x_i)\\ &\leq C\exp(-(a^*\varepsilon_2/\varepsilon_1)\sigma_1)\\ &\leq CN^{-1}.\end{aligned}$$

Hence, for $x_i \in [\sigma_1, 1]$

$$\left|V^{n+1}(x_i) - \widetilde{V}_i\right| \leq CN^{-1}. \tag{6.13}$$

Finally, on combining (6.12) and (6.13), we get

$$\left\|V^{n+1}(x_i) - \widetilde{V}_i\right\|_{\Omega^N} \leq CN^{-1}(\ln N)^2,\ \forall x_i \in \Omega^N. \qquad \square$$

Lemma 6.4.5. *The error bound for the right singular component is given by*

$$\left\|W^{n+1}(x_i) - \widetilde{W}_i\right\|_{\Omega^N} \leq CN^{-1}\ln N.$$

Proof. For the uniform mesh, the proof is similar as for the left singular component. In the second case $\sigma_1, \sigma_2 < 1/4$ for $x_i \in [0, 1-\sigma_2)$, we have

$$\left|W^{n+1}(x_i) - \widetilde{W}_i\right| \leq \left|W^{n+1}(x_i)\right| + \left|\widetilde{W}_i\right|.$$

Using Theorem 6.4.1, we obtain

$$\left|\widetilde{W}_{3N/4}\right| \leq C(1 + 4N^{-1}\ln N)^{-N/4}.$$

Now for $x = 4N^{-1}\ln N$ the inequality $\ln(1+x) > x(1-x/2)$ gives $\left|\widetilde{W}_i\right| \leq CN^{-1}$, $\forall x_i \in [0, 1-\sigma_2)$. Also,

$$\begin{aligned}\left|W^{n+1}(x_i)\right| &\leq C\exp(-(b^*/\varepsilon_2)(1-x_i)) \\ &\leq C\exp(-(b^*/\varepsilon_2)\sigma_2) \\ &\leq CN^{-2}.\end{aligned}$$

Hence, for $x_i \in [0, 1-\sigma_2)$

$$\left|W^{n+1}(x_i) - \widetilde{W}_i\right| \leq CN^{-1}. \tag{6.14}$$

Now for $x_i \in [1-\sigma_2, 1]$, the classical argument gives

$$\begin{aligned}\left|\mathscr{L}^N\left(W^{n+1}(x_i) - \widetilde{W}_i\right)\right| &\leq C\left(\varepsilon_1 H_3^2\left|W^{n+1}(x_i)\right|_4 + \varepsilon_2 H_3\|a\|\left|W^{n+1}(x_i)\right|_2\right) \\ &\leq C\left(\varepsilon_1\sigma_2^2 N^{-2}\left|W^{n+1}(x_i)\right|_4 + \varepsilon_2\sigma_2 N^{-1}\|a\|\left|W^{n+1}(x_i)\right|_2\right) \\ &\leq CN^{-1}\ln N. \end{aligned}\tag{6.15}$$

Finally, on combining (6.14) and (6.15), we get

$$\left\|W^{n+1}(x_i) - \widetilde{W}_i\right\|_{\Omega^N} \leq CN^{-1}\ln N. \qquad \square$$

Analysis for Case II ($\varepsilon_2^2/\varepsilon_1 \to 0$ as $\varepsilon_1 \to 0$). In this case, we decompose the solution $\widetilde{\psi}_i$ of (6.3) as

$$\widetilde{\psi}_i = \widetilde{\chi}_i + \widetilde{Z}_i,$$

where $\widetilde{\chi}_i$ and $\widetilde{Z}_i$ (the regular and singular components respectively) satisfy the following inhomogeneous and homogeneous problems respectively

$$\begin{aligned}&\mathscr{L}^N\widetilde{\chi}_i = \widetilde{g}(x_i) \text{ in } R^{N,M}, \quad \widetilde{\chi}_i = \chi^{n+1}(x_i) \text{ on } \Gamma^{N,M}, \\ &\mathscr{L}^N\widetilde{Z}_i = 0 \text{ in } R^{N,M}, \quad \widetilde{Z}_i = Z^{n+1}(x_i) \text{ on } \Gamma^{N,M}.\end{aligned}$$

The nodal error is given by

$$v_{i,j+1} = \psi^{n+1}(x_i) - \widetilde{\psi}_i = \left(\chi^{n+1}(x_i) - \widetilde{\chi}_i\right) + \left(Z^{n+1}(x_i) - \widetilde{Z}_i\right).$$

Theorem 6.4.2. *The bounds on the singular component are given by*

$$\left|\widetilde{Z}_i\right| \leq C\prod_{j=1}^{i}\left(1+\mu_1 h_j\right)^{-1},\ \left|\widetilde{Z}_0\right| \leq C,\ \left|\widetilde{Z}_N\right| \leq C.$$

Proof. The proof can be done by following the approach given in [105]. □

Lemma 6.4.6. *The error bound for the regular component is given by*

$$\left\|\chi^{n+1}(x_i)-\widetilde{\chi}_i\right\|_{\Omega^N} \leq CN^{-2}.$$

Proof. Using the bounds for χ^{n+1}, the proof is similar as Lemma 6.4.3. □

Lemma 6.4.7. *The error bound for the singular component is given by*

$$\left\|Z^{n+1}(x_i)-\widetilde{Z}_i\right\|_{\Omega^N} \leq CN^{-2}(\ln N)^2.$$

Proof. We consider the uniform mesh and the non-uniform meshes separately. For the uniform mesh *i.e.,* in the case $\sigma_1=\sigma_2=1/4$ the classical argument yields

$$\begin{aligned}\left|\mathscr{L}^N\left(Z^{n+1}(x_i)-\widetilde{Z}_i\right)\right| &= \left|\mathscr{L}^N Z^{n+1}(x_i)-0\right| \\ &= \left|\left(\mathscr{L}^N-\hat{L}\right)Z^{n+1}(x_i)\right| \\ &\leq C\left(\varepsilon_1 N^{-2}\left|Z^{n+1}(x_i)\right|_4+\varepsilon_2 N^{-1}\|a\|\left|Z^{n+1}(x_i)\right|_2\right) \\ &\leq CN^{-2}(\ln N)^2.\end{aligned}$$

In the latter case depending on the mesh spacing, a different argument is used to obtain the error estimate. For $x_i\in[\sigma_1,1-\sigma_1]$, we have

$$\left|Z^{n+1}(x_i)-\widetilde{Z}_i\right| \leq \left|Z^{n+1}(x_i)\right|+\left|\widetilde{Z}_i\right|.$$

Now using Theorem 6.4.2, we obtain

$$\left|\widetilde{Z}_{N/4}\right| \leq C\left(\left(1+4N^{-1}\ln N\right)^{-N/8}\right)^2.$$

Now for $x = 4N^{-1}\ln N$ the inequality $\ln(1+x) > x(1-x/2)$ gives $\left|\widetilde{Z}_i\right| \leq CN^{-2}$, $\forall x_i \in [\sigma_1, 1-\sigma_1]$. Also,

$$\begin{aligned}\left|Z^{n+1}(x_i)\right| &\leq C\exp\left((-\sqrt{\gamma b^*/\varepsilon_1}\right))x_i \\ &\leq C\exp\left((-\sqrt{\gamma b^*/\varepsilon_1}\right)\sigma_1) \\ &\leq CN^{-2}.\end{aligned}$$

Hence for $x_i \in [\sigma_1, 1-\sigma_1]$, we obtain

$$\left|Z^{n+1}(x_i) - \widetilde{Z}_i\right| \leq CN^{-2}. \tag{6.16}$$

Now if $x_i \in [0, \sigma_1)$, then

$$\begin{aligned}\left|\mathscr{L}^N\left(Z^{n+1}(x_i) - \widetilde{Z}_i\right)\right| &\leq C\left(\varepsilon_1 H_1^2\left|Z^{n+1}(x_i)\right|_4 + \varepsilon_2 H_1\|a\|\left|Z^{n+1}(x_i)\right|_2\right) \\ &\leq C\left(\varepsilon_1\sigma_1^2 N^{-2}\left|Z^{n+1}(x_i)\right|_4 + \varepsilon_2\sigma_1 N^{-1}\|a\|\left|Z^{n+1}(x_i)\right|_2\right) \\ &\leq CN^{-2}(\ln N)^2.\end{aligned}$$

Thus using Lemma 6.4.2, we get the following estimate

$$\left|Z^{n+1}(x_i) - \widetilde{Z}_i\right| \leq CN^{-2}(\ln N)^2.$$

Similar bound can be obtained for the interval $[1-\sigma_1, 1]$. Hence,

$$\left\|Z^{n+1}(x_i) - \widetilde{Z}_i\right\|_{\Omega^N} \leq CN^{-2}(\ln N)^2,\ \forall x_i \in \Omega^N. \qquad \square$$

Theorem 6.4.3. *The solution $\psi(x,t)$ of the continuous problem and the solution $\widetilde{\psi}_i$ of the fully discretized scheme satisfy the following parameter-uniform error estimate*

$$\sup_{0<\varepsilon_1,\varepsilon_2\ll 1}\|\psi(x_i,t_n) - \widetilde{\psi}_i\| = \sup_{0<\varepsilon_1,\varepsilon_2\ll 1}\left(\max_n\left(\max_i|\psi(x_i,t_n) - \widetilde{\psi}_i|\right)\right)$$

$$\leq C\begin{cases}\left((\Delta t)^2 + N^{-1}(\ln N)^2\right), & \textit{Case I},\\ \left((\Delta t)^2 + N^{-2}(\ln N)^2\right), & \textit{Case II}.\end{cases}$$

Proof. The proof follows from the triangle inequality and Lemmas 6.3.3, 6.4.3, 6.4.4, 6.4.5, 6.4.6 and 6.4.7. $\square$

6.5 Numerical Illustrations

The unavailability of the exact/analytical solution to the test problems suggest us to use the double mesh principle [8] to check the accuracy of the method in terms of the maximum absolute errors. For each ε_1 and ε_2, the maximum absolute error is calculated as

$$e^{N,M}_{\varepsilon_1,\varepsilon_2} = \max_n \left(\max_i \left| \widetilde{\psi}^{2N,2M}_{2i} - \widetilde{\psi}^{N,M}_i \right| \right),$$

where $\widetilde{\psi}^{N,M}_i$ and $\widetilde{\psi}^{2N,2M}_{2i}$ are the numerical solutions on $R^{N,M}$ and $R^{2N,2M}$ respectively. Note that the value of σ_1 and σ_2 are different in the case of N and $2N$ mesh intervals in the spatial direction, and so the comparison of the solutions using the double mesh principle will not be accurate. To overcome this issue, a fine mesh $R^{2N,2M}$ is obtained by the mesh $R^{N,M}$ by using the interpolation. The parameters uniform point-wise error is estimated by taking the maximum of $e^{N,M}_{\varepsilon_1,\varepsilon_2}$ over several values of ε_1 and ε_2 *i.e.,*

$$e^{N,M} = \max_{\varepsilon_1,\varepsilon_2} e^{N,M}_{\varepsilon_1,\varepsilon_2}.$$

Moreover, the order of convergence $\rho^{N,M}_{\varepsilon_1,\varepsilon_2}$ and the parameters-uniform order of convergence $\rho^{N,M}$ of the proposed method are calculated as

$$\rho^{N,M}_{\varepsilon_1,\varepsilon_2} = \log_2 \left(\frac{e^{N,M}_{\varepsilon_1,\varepsilon_2}}{e^{2N,2M}_{\varepsilon_1,\varepsilon_2}} \right), \text{ and } \rho^{N,M} = \log_2 \left(\frac{e^{N,M}}{e^{2N,2M}} \right).$$

Example 6.5.1.

$$-\frac{\partial \psi(x,t)}{\partial t} + \varepsilon_1 \frac{\partial^2 \psi(x,t)}{\partial x^2} + \varepsilon_2(1+x)\frac{\partial \psi(x,t)}{\partial x} - \psi(x,t) = -x^2 - 1,\ (x,t) \in R,$$
$$\psi(x,0) = 1 - x^2,\ 0 \le x \le 1,$$
$$\psi(0,t) = 1 + t,\ \psi(1,t) = 0,\ 0 \le t \le 1.$$

Example 6.5.2.

$$
\begin{aligned}
-\frac{\partial \psi(x,t)}{\partial t} + \varepsilon_1 \frac{\partial^2 \psi(x,t)}{\partial x^2} + \varepsilon_2 (1+xt) \frac{\partial \psi(x,t)}{\partial x} - (1+t)\psi(x,t) \\
= -\exp(-t)(x+1), (x,t) \in R, \\
\psi(x,0) = \sin(\pi x),\ 0 \le x \le 1, \\
\psi(0,t) = 0,\ \psi(1,t) = 0,\ 0 \le t \le 1.
\end{aligned}
$$

Table 6.1: Computational results for Example 6.5.1 for $\varepsilon_1 = 2^{-10}$ and different values of ε_2.

	Number of intervals N					
ε_2	32	64	128	256	512	1024
2^{-10}	9.58e-03	6.85e-03	3.55e-03	1.44e-03	4.86e-04	1.28e-04
	0.48	0.95	1.30	1.57	1.92	
2^{-11}	9.53e-03	6.81e-03	3.54e-03	1.44e-03	4.84e-04	1.28e-04
	0.48	0.94	1.30	1.57	1.92	
2^{-12}	9.50e-03	6.79e-03	3.53e-03	1.44e-03	4.83e-04	1.27e-04
	0.48	0.94	1.29	1.58	1.93	
2^{-13}	9.49e-03	6.78e-03	3.52e-03	1.43e-03	4.83e-04	1.27e-04
	0.48	0.94	1.30	1.56	1.93	
2^{-14}	9.48e-03	6.78e-03	3.52e-03	1.43e-03	4.82e-04	1.27e-04
	0.48	0.94	1.30	1.57	1.92	
2^{-15}	9.48e-03	6.78e-03	3.52e-03	1.43e-03	4.82e-04	1.27e-04
	0.48	0.95	1.30	1.57	1.92	
$\vdots$	$\vdots$	$\vdots$	$\vdots$	$\vdots$	$\vdots$	
2^{-22}	9.47e-03	6.77e-03	3.52e-03	1.43e-03	4.82e-04	1.27e-04
	0.48	0.94	1.30	1.57	1.92	
$e^{N,M}$	9.58e-03	6.85e-03	3.55e-03	1.44e-03	4.86e-04	1.28e-04
$\rho^{N,M}$	0.48	0.95	1.30	1.57	1.92	

Table 6.2: Computational results for Example 6.5.1 for $\varepsilon_2 = 2^{-12}$ and different values of ε_1.

	Number of intervals N					
ε_1	32	64	128	256	512	1024
2^{-26}	2.21e01	8.27e-02	4.12e-02	2.14e-02	1.15e-02	6.36e-03
	1.42	1.00	0.95	0.90	0.85	
2^{-30}	2.18e-01	1.21e-01	6.91e-02	3.87e-02	2.13e-02	1.16e-02
	0.85	0.81	0.84	0.86	0.88	
2^{-34}	2.32e-01	1.29e-01	7.53e-02	4.30e-02	2.42e-02	1.34e-02
	0.85	0.78	0.81	0.83	0.85	
2^{-38}	2.88e-01	1.30e-01	7.57e-02	4.33e-02	2.44e-02	1.35e-02
	1.15	0.78	0.81	0.83	0.85	
2^{-42}	3.58e-01	1.37e-01	7.57e-02	4.33e-02	2.44e-02	1.35e-02
	1.39	0.86	0.81	0.83	0.85	
2^{-46}	3.64e-01	1.49e-01	7.57e-02	4.33e-02	2.44e-02	1.35e-02
	1.29	0.98	0.81	0.83	0.85	
$e^{N,M}$	3.64e-01	1.49e-01	7.57e-02	4.33e-02	2.44e-02	1.35e-02
$\rho^{N,M}$	1.29	0.98	0.81	0.83	0.85	

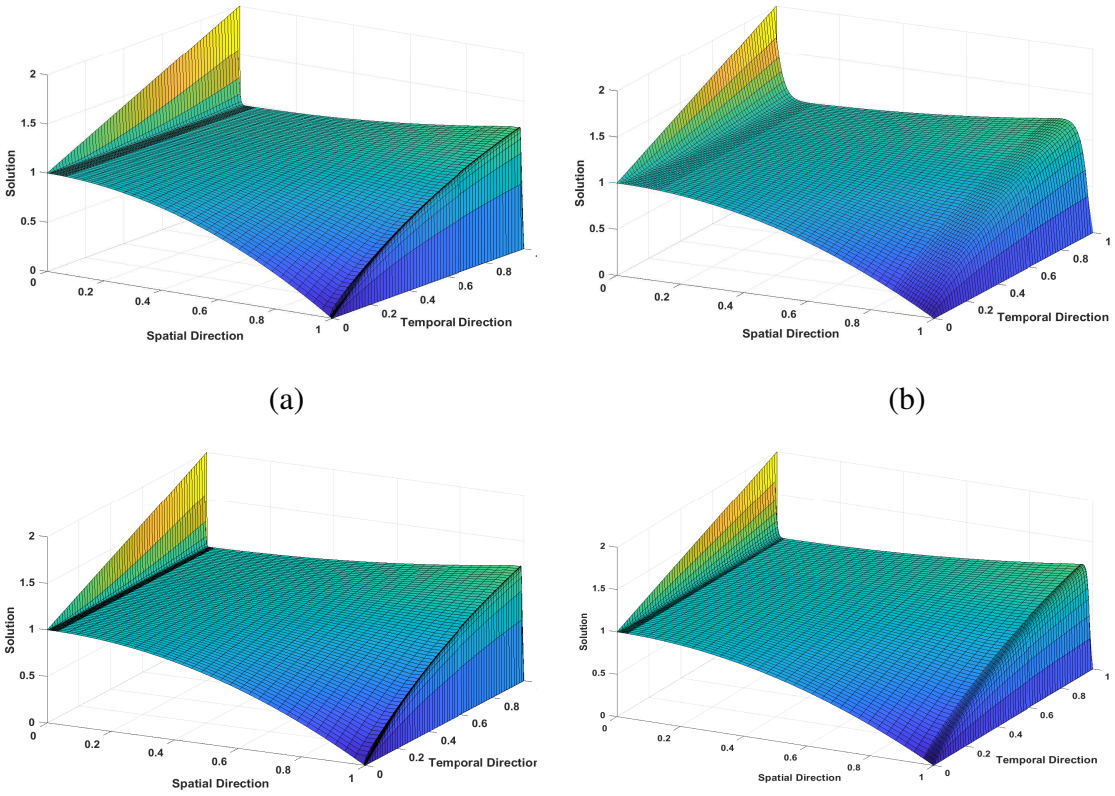

Figure 6.1: Numerical solution profiles for Example 6.5.1 for (a) $\varepsilon_1 = 2^{-15}$, $\varepsilon_2 = 2^{-6}$ (b) $\varepsilon_1 = 2^{-10}$, $\varepsilon_2 = 2^{-8}$ (c) $\varepsilon_1 = 2^{-17}$, $\varepsilon_2 = 2^{-7}$ and (d) $\varepsilon_1 = 2^{-14}$, $\varepsilon_2 = 2^{-18}$.

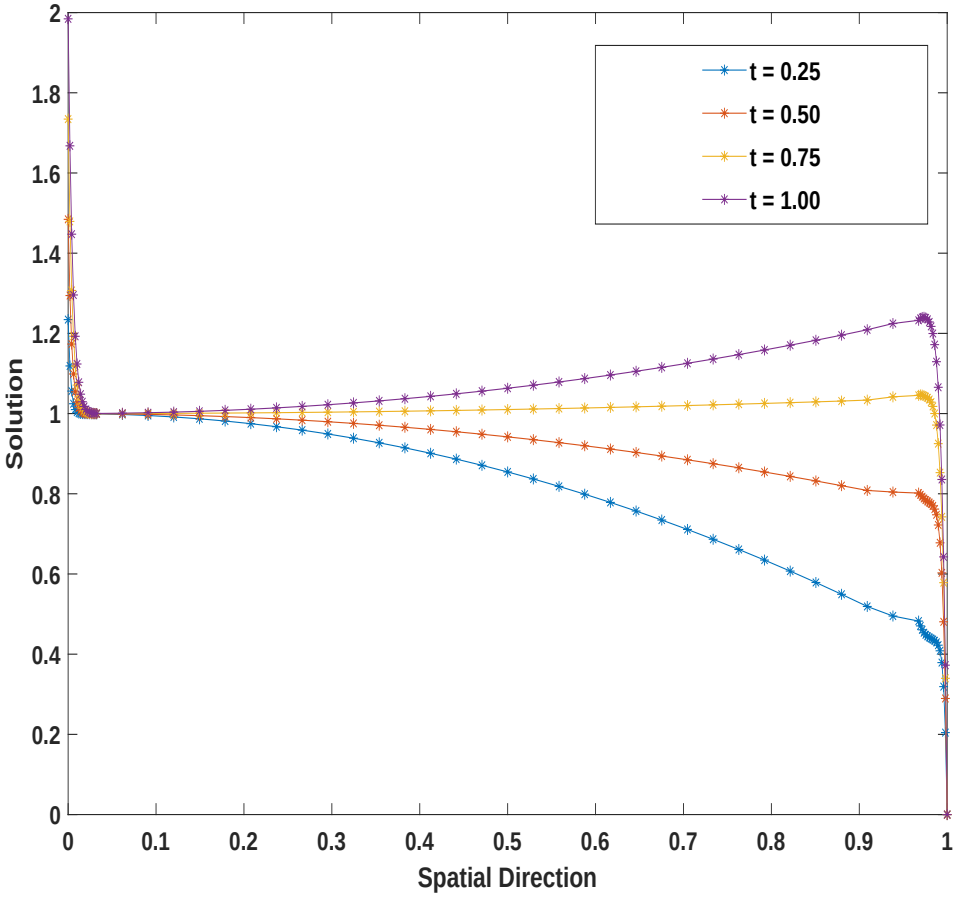

Figure 6.2: Numerical solution profiles for Example 6.5.1 for $\varepsilon_1 = 2^{-14}$, $\varepsilon_2 = 2^{-18}$.

Table 6.3: Computational results for Example 6.5.2 for $\varepsilon_1 = 2^{-10}$ and different values of ε_2.

	Number of intervals N					
ε_2	32	64	128	256	512	1024
2^{-10}	1.29e-02	1.02e-02	5.49e-03	2.24e-03	7.44e-04	2.09e-04
	0.34	0.89	1.29	1.59	1.83	
2^{-11}	1.29e-02	1.02e-02	5.47e-03	2.24e-03	7.42e-04	2.10e-04
	0.34	0.89	1.29	1.59	1.82	
2^{-12}	1.28e-02	1.02e-02	5.46e-03	2.23e-03	7.41e-04	2.11e-04
	0.33	0.90	1.29	1.59	1.81	
2^{-13}	1.28e-02	1.01e-02	5.45e-03	2.23e-03	7.41e-04	2.11e-04
	0.34	0.89	1.29	1.59	1.81	
2^{-14}	1.28e-02	1.01e-02	5.45e-03	2.23e-03	7.40e-04	2.11e-04
	0.34	0.89	1.29	1.59	1.81	
2^{-15}	1.28e-02	1.01e-02	5.45e-03	2.23e-03	7.40e-04	2.11e-04
	0.34	0.89	1.29	1.59	1.81	
$\vdots$	$\vdots$	$\vdots$	$\vdots$	$\vdots$	$\vdots$	
2^{-22}	1.28e-02	1.01e-02	5.44e-03	2.23e-03	7.40e-04	2.11e-04
	0.34	0.89	1.29	1.59	1.81	
$e^{N,M}$	1.29e-02	1.02e-02	5.49e-03	2.24e-03	7.44e-04	2.11e-04
$\rho^{N,M}$	0.34	0.89	1.29	1.59	1.82	

Table 6.4: Computational results for Example 6.5.2 for $\varepsilon_2 = 2^{-12}$ and different values of ε_1.

	Number of intervals N					
ε_1	32	64	128	256	512	1024
2^{-26}	9.91e-02	3.60e-02	1.84e-02	1.13e-02	7.84e-03	5.06e-03
	1.46	0.97	0.70	0.53	0.63	
2^{-30}	2.63e-01	1.36e-01	7.06e-02	3.70e-02	1.94e-02	1.01e-02
	0.95	0.95	0.93	0.93	0.94	
2^{-34}	3.66e-01	1.86e-01	9.37e-02	4.70e-02	2.36e-02	1.18e-02
	0.98	0.99	1.00	0.99	1.00	
2^{-38}	3.76e-01	1.92e-01	9.70e-02	4.87e-02	2.44e-02	1.22e-02
	0.97	0.99	0.99	1.00	1.00	
2^{-42}	3.77e-01	1.93e-01	9.72e-02	4.88e-02	2.45e-02	1.22e-02
	0.97	0.99	0.99	0.99	1.00	
2^{-46}	3.77e-01	1.93e-01	9.72e-02	4.88e-02	2.45e-02	1.22e-02
	0.97	0.99	0.99	0.99	1.00	
$e^{N,M}$	3.77e-01	1.93e-01	9.72e-02	4.88e-02	2.45e-02	1.22e-02
$\rho^{N,M}$	0.97	0.99	0.99	0.99	1.00	

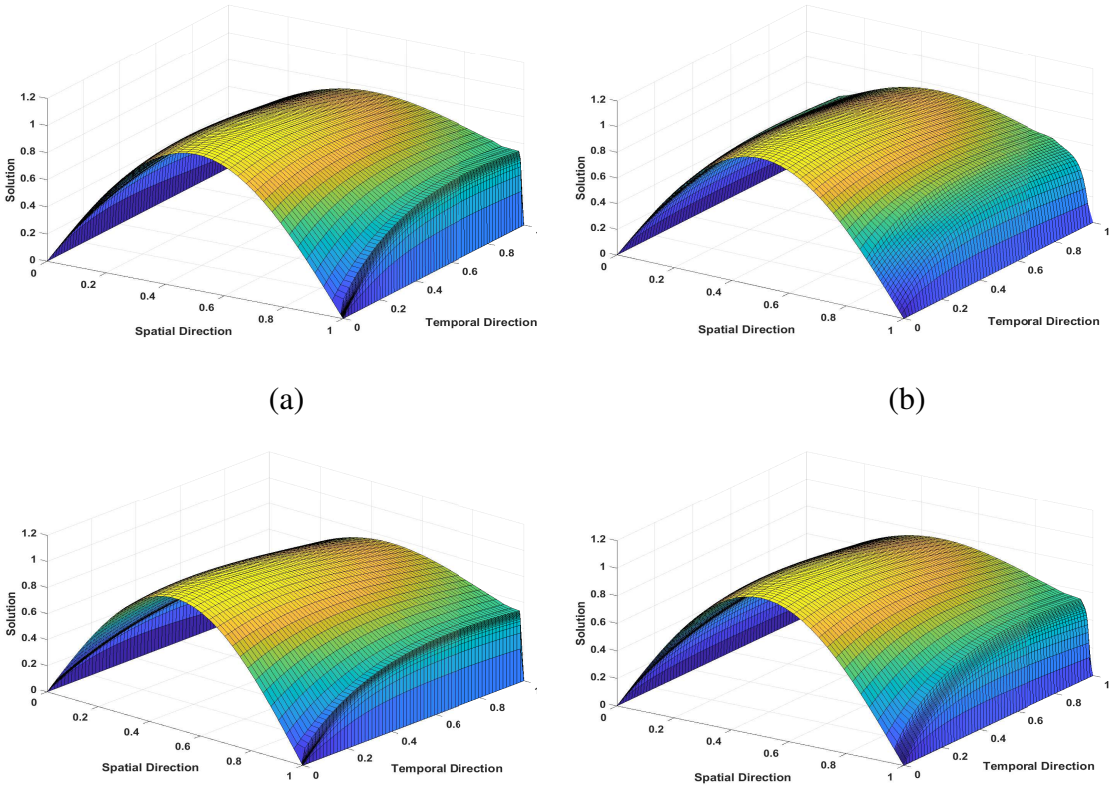

Figure 6.3: Numerical solution profiles for Example 6.5.2 (viewed from right) for (a) $\varepsilon_1 = 2^{-15},\ \varepsilon_2 = 2^{-6}$ (b) $\varepsilon_1 = 2^{-10},\ \varepsilon_2 = 2^{-8}$ (c) $\varepsilon_1 = 2^{-17},\ \varepsilon_2 = 2^{-7}$ and (d) $\varepsilon_1 = 2^{-14},\ \varepsilon_2 = 2^{-18}$.

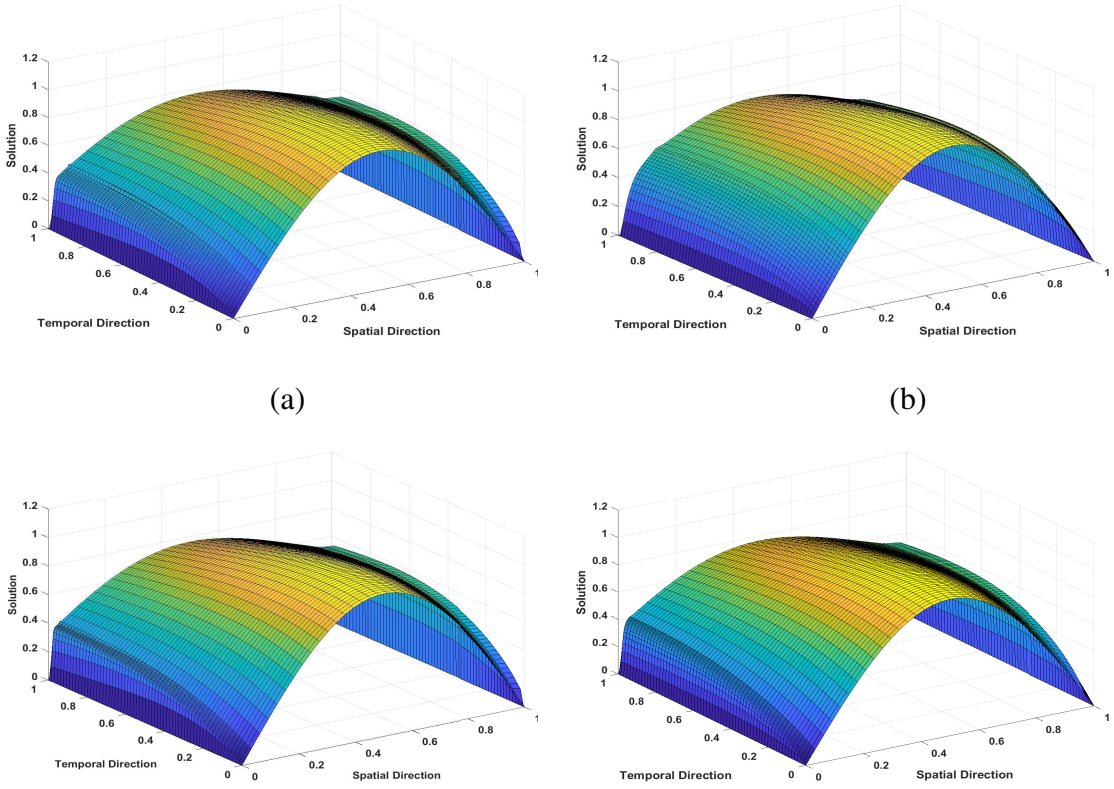

Figure 6.4: Numerical solution profiles for Example 6.5.2 (viewed from left) for (a) $\varepsilon_1 = 2^{-15}$, $\varepsilon_2 = 2^{-6}$ (b) $\varepsilon_1 = 2^{-10}$, $\varepsilon_2 = 2^{-8}$ (c) $\varepsilon_1 = 2^{-17}$, $\varepsilon_2 = 2^{-7}$ and (d) $\varepsilon_1 = 2^{-14}$, $\varepsilon_2 = 2^{-18}$.

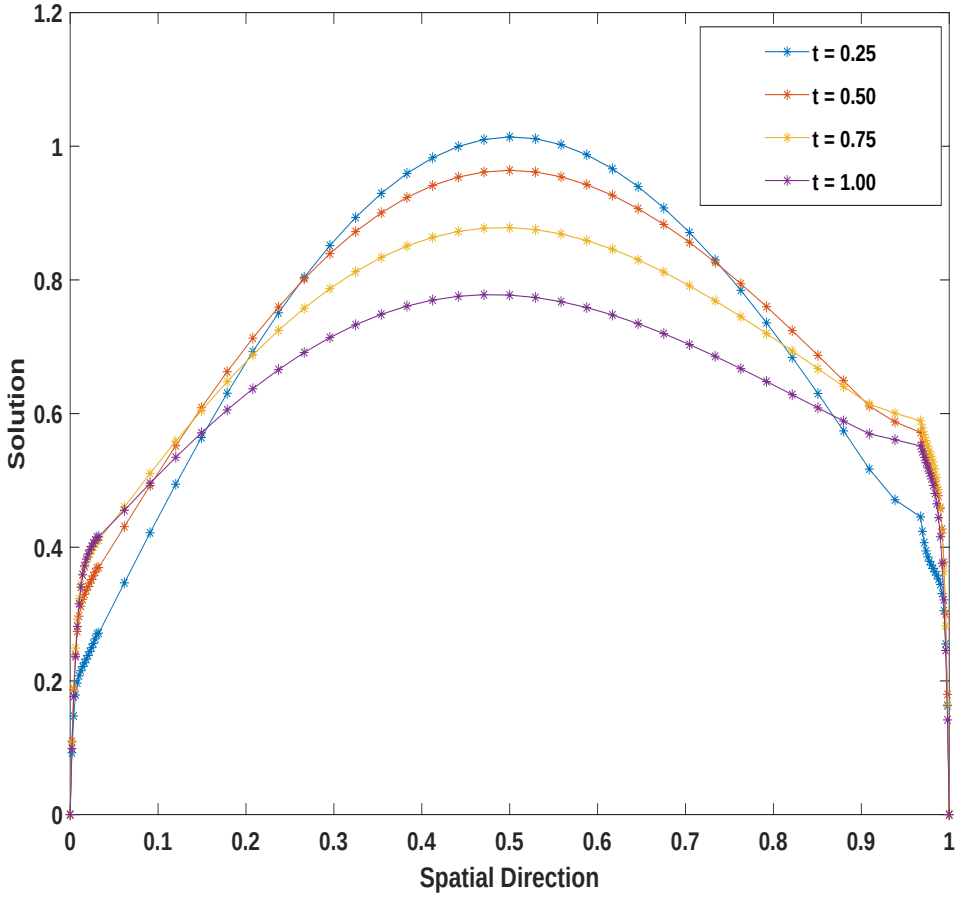

Figure 6.5: Numerical solution profiles for Example 6.5.2 for $\varepsilon_1 = 2^{-14}$, $\varepsilon_2 = 2^{-18}$.

To verify theoretical estimates, the numerical results are presented in this section. For the test examples, the results are obtained on a wide range $\mathscr{R}(\varepsilon_1, \varepsilon_2)$ of perturbation parameters satisfying Case I or Case II and the mesh is of Shishkin type. Note that the case $\sigma_1, \sigma_2 \geq 1/4$ occur for a small range $\mathscr{R}(\varepsilon_1, \varepsilon_2)$ of perturbation parameters, and the uniform mesh is sufficient to obtain good accuracy. We performed our experiments for both cases, in Case I, our problem is similar to the convection-diffusion problem, while in Case II, it becomes similar to the reaction-diffusion problem. The results presented in the Tables 6.1-6.4 confirm the error estimates when applied to the Shishkin-type mesh. In Tables 6.1 and 6.3 for a fixed ε_1, the maximum absolute error becomes stable as $\varepsilon_2 \to 0$. This shows that the method is ε_2-uniform convergent. The ε_1-uniform convergence is confirmed from Tables 6.2, 6.2 and 6.4 where for a fixed ε_2, the maximum absolute error becomes stable as $\varepsilon_1 \to 0$. The results presented

in Tables 6.1, 6.2, 6.3 and 6.4 are obtained by taking $M = N$, while, to show that the dominating error is in the spatial direction the results presented in Table 6.2 are obtained by taking $M = N/2$.

For both test problems, for different values of $\varepsilon_1, \varepsilon_2$, the physical phenomenon of the solution are presented in the form of the surface plots (refer Figs. 6.1-6.4). These graphs clearly indicate that for small perturbation parameters close to zero, the solution of the test problems exhibit parabolic boundary layers at both lateral surfaces, and the boundary layer width continuously depends on these parameters. The layer phenomenon and the effect of $\varepsilon_1, \varepsilon_2$ can also be observed from the graphs for different time levels (refer Figs. 6.2 and 6.5). To plot all the graphs, we have used $M = N = 64$.

6.6 Conclusion

To approximate the solution of two-parameter singularly perturbed parabolic problems, we have proposed an implicit numerical scheme on a Shishkin-type mesh. Rigorous convergence analysis for both cases $\varepsilon_1/\varepsilon_2^2 \to 0$ as $\varepsilon_2 \to 0$ and $\varepsilon_2^2/\varepsilon_1 \to 0$ as $\varepsilon_1 \to 0$ are given separately. It has been shown that the proposed scheme is second-order accurate in time in both cases while it is first-order and second-order accurate in space in Case I and Case II, respectively. The effect of the parameters ε_1 and ε_2 on the solution behaviour is shown graphically. The very high gradients near both boundaries $x = 0$ and $x = 1$ can be noticed for small ε_1 and ε_2. Also, we noticed that the numerical results presented in the tables meet the theoretical error bounds very well. For the future reference, one can include the convergence analysis in the different norm like energy norm, L_1 norm, and L_2 norm, etc (for the importance of the norms the readers are referred to [132]). Moreover, depending on the method used, one may get different rate of convergence in different norms (see [104] for the reference, where it is shown that the Galerkin method on a B-type mesh is first-order accurate in the energy norm while it is second-order accurate in the maximum norm). One may also look into the development of other types of layer-adapted meshes like Bakhvalov mesh, Bakhvalov-Shishkin mesh, etc. An extension of the proposed scheme on the different problems like higher-dimensional problems, the system of equations, etc. can also be explored.